Thermodynamics of anisotropic superconducting indium analyzed in terms of Eliashberg theory

L. Niel, N. Giesinger, and H. W. Weber
Atominstitut der Österreichischen Universitäten, A-1020 Wien, Austria

E. Schachinger
Institut für Theoretische Physik, Technische Universität, A-8010 Graz, Austria

(Received 25 January 1985)

Experiments on the change of thermodynamic properties with impurity concentration in indium are presented, which cover the temperature range from 30 mK to the superconducting transition temperature T_c. From an analysis of the T_c depression with impurity concentration and the temperature dependence of the thermodynamic critical fields in terms of Eliashberg theory, we conclude that the electron-phonon coupling anisotropy is large in indium. The mean-square anisotropy parameter $\langle a^2 \rangle$ of the usual separable pairing potential is found to be 0.035—0.040. Particular attention is paid to the influence of various experimental error sources and the role of input parameters on the theoretical analysis. It is shown that the concept of coupling anisotropy and anisotropy removal by impurity scattering provides the only consistent description of the experimental results.

I. INTRODUCTION

Anisotropy effects in the superconducting state have been a challenge to theorists as well as experimentalists for many years. Starting from the "isotropic" BCS theory of superconductivity, Anderson[1] and, in more detail, Markowitz and Kadanoff[2] introduced a separable pairing potential $V(\mathbf{k},\mathbf{k}')=(1+a_{\mathbf{k}})V_{\mathrm{BCS}}(1+a_{\mathbf{k}'})$, where $a_{\mathbf{k}}$ is the temperature independent anisotropy parameter and V_{BCS} is the constant potential of the BCS theory. According to their definition, the average of the anisotropy parameter over the entire Fermi surface is zero, the mean-square anisotropy parameter $\langle a^2 \rangle$, which denotes the average of $a_{\mathbf{k}}^2$ over the Fermi surface, expresses the average deviation of the coupling from the isotropic case. Therefore $\langle a^2 \rangle$ comprises in a rather simple way anisotropies of the electron system, the phonon spectra, and the electron-phonon interaction. An immediate result of this theory is the enhancement of the transition temperature T_c by a few percent due to the anisotropy of the energy gap. This result refers to the clean limit (electron mean free path $l=\infty$); the addition of small amounts of nonmagnetic impurities continuously reduces the anisotropy effect and, hence, T_c by the introduction of additional scattering centers, which provide new k states and, therefore, tend to smear out the original distribution of states.

An extension of this work was made by Clem,[3] who calculated the influence of anisotropy effects on the thermodynamic properties of superconductors, in particular the thermodynamic critical field $H_c(T)$ and the deviation function $D(t)$. Of course, all of these calculations are restricted to the weak-coupling limit only. Strong-coupling effects, which also change T_c and $H_c(T)$ in a significant way, were treated in a more phenomenological way[4,5] by introducing a second "fit" parameter δ, in order to separate the competing effects of anisotropy and strong coupling in the case of the deviation function.

A full theoretical treatment of anisotropic superconductors with arbitrary coupling strength based on the solution of Eliashberg theory became available only fairly recently.[6–9] Although the numerical solution of these equations in their anisotropic form requires a significant amount of computer capacity, the theory in the present form (in particular, if combined with the Fermi-surface harmonics notation introduced by Butler and Allen[10]) represents an ideal tool for the analysis and interpretation of experiments on the thermodynamics of anisotropic superconductors.

Considering the experimental situation, two distinctly different approaches are feasible. In the first approach, experimental techniques are applied, which map directly the direction dependence of certain superconducting properties in single crystalline materials (e.g., H_{c2}, flux line lattice, ultrasound absorption, tunneling characteristics, etc.), whereas in the second approach the integral effect of anisotropy on the superconducting properties is determined [e.g., the T_c depression by impurity or boundary scattering, the thermodynamic critical field $H_c(T)$ and the electronic specific heat in the superconducting state]. For an overview of experimental techniques and their evaluation we refer to the paper by Bostock and Mac Vicar.[11] Clearly, all of the experiments belonging to the first group have the advantage of providing direct access to the magnitude of the anisotropy effect. However, because the theoretical situation is not satisfactory yet (cf., e.g., Ref. 12), the interpretation of results in terms of electron-phonon coupling anisotropy is difficult or impossible at the present stage. On the contrary, if careful experiments on the thermodynamics of superconductors are combined with the full analysis in terms of Eliashberg theory, an unambiguous determination of the mean-square coupling anisotropy seems to be feasible (concerning a first attempt of this type, cf. Ref. 13).

In the following we wish to present an analysis along

these lines for the type-I superconductor In and a series of InTl alloys. The experiments are presented in Sec. II and a brief outline of the theory is given in Sec. III. Section IV deals with the analysis of the experimental data, where particular attention is paid to the influence of various input parameters on the results obtained from Eliashberg theory. Finally, the conclusions of our analysis are presented in Sec. V.

II. EXPERIMENTAL

Our choice of In as the superconducting system to be investigated with respect to the T_c depression by the addition of impurities and the temperature dependence of the thermodynamic critical field relied on several considerations:[5,14–18] First, indium—if alloyed with Tl—remains a type-I superconductor up to fairly high Tl concentrations ($\sim$20 at. %), which greatly facilitates the experimental determination of the thermodynamic critical fields; second, because of their similar electronic structures the differences in electronegativity between In and Tl are minimal (1.7 and 1.8, respectively[18]), which allows one to neglect valence effects on the change of T_c; third, low-temperature specific-heat and electron-phonon interaction data calculated from tunneling experiments are available for several alloys, which provide information on the density of states $N(0)$ and the spectral function $\alpha^2F(\omega)$ needed for the theoretical analysis; fourth, the spectral functions $\alpha^2F(\omega)$ of In and $In_{90}Tl_{10}$ are almost identical (cf. Fig. 6); and fifth, both indium and thallium can be obtained readily at a very high-purity level.

The polycrystalline samples were prepared from 99.9999%-purity (In) and 99.999%-purity (Tl) starting materials, respectively, whose content of magnetic impurities was checked by x-ray fluorescence analysis and found to be smaller than 1 ppm in both cases. The alloys were prepared by carefully weighing the desired amounts of material, etching them several times to remove oxide layers and melting them under an overpressure of argon at temperatures between 160 °C and 300 °C. Then the samples were cast to their final cylindrical form (3 mm cross sectional diameter, 20 mm length) and stored under an argon atmosphere. The Tl content of the lowest-concentration samples was checked again by x-ray fluorescence analysis and found to agree with the nominal composition to within $\pm$0.1 at. %.

The experiments were made in a conventional bath cryostat in the temperature range from 1.6 K to the transition temperature and in a dilution refrigerator from 30 mK to about 2 K. In both cases the ac susceptibility of the samples was measured by superimposing a small ac ripple field (10—100 μT) on a transverse dc field, which was provided either by a superconducting magnet in the bath cryostat or by an electromagnet in the dilution refrigerator, and by detecting the pick-up voltages with a lock-in amplifier. The transverse geometry was chosen in order to avoid the formation of a superconducting surface sheath for samples with $\kappa > 0.42$.

The transition widths at T_c, which were determined by sweeping the temperature in the absence of an external field through T_c, were found to be very small ($\sim$3 mK) in all samples indicating a truly homogeneous distribution of Tl atoms in the alloys. Concerning the determination of $H_c(T)$ extremely slow sweep times of the external field had to be used (1.5—35 μT s^{-1}) in order to obtain reproducible, i.e., sweep-time independent, results on the transition field. At constant temperature ($\pm$0.5 mK) the data in either increasing or decreasing fields could typically be reproduced to within 10 μT, the difference between these two branches varied between 100 and 500 μT (cf. Fig. 1). For all further evaluations the transition in increasing fields was used.

Whereas the relative accuracy of the temperature as well as the field measurement is clearly satisfactory, some considerations on the absolute values of temperature and field seem to be appropriate. For the temperature measurement calibrated Ge resistors were used, whose maximum error according to their specification was about 4 mK near 4 K. Calibration of one resistor against a standard lead sample yielded $T_c = (7.2018 \pm 0.0018)$ K, which agrees with the standard T_c value of 7.200 K within the error limits, but is too high by 1.8 mK. Measurements of $H_c(T)$ near T_c with this resistor as the temperature sensor, and identical experiments in another cryostat using a different resistor and magnetic field supply agreed to within 4 mK with respect to the result on T_c. Similar agreement was obtained for $H_c(T)$ between the experiments in the bath cryostat and the dilution refrigerator in the overlapping temperature range (1.6—2.0 K), where again another Ge resistor and magnetic field supply were used. From these crosschecks we believe, that the temperatures and, in particular, the T_c values are accurate to better than $\pm$2 mK on an absolute scale. Concerning the magnetic fields, calibrations with a high-resolution temperature-stabilized Hall probe were made at the position of the sample. Again excellent agreement on $H_c(T)$ between the two setups was obtained, but a quantitative estimate of the absolute accuracy is difficult. From a

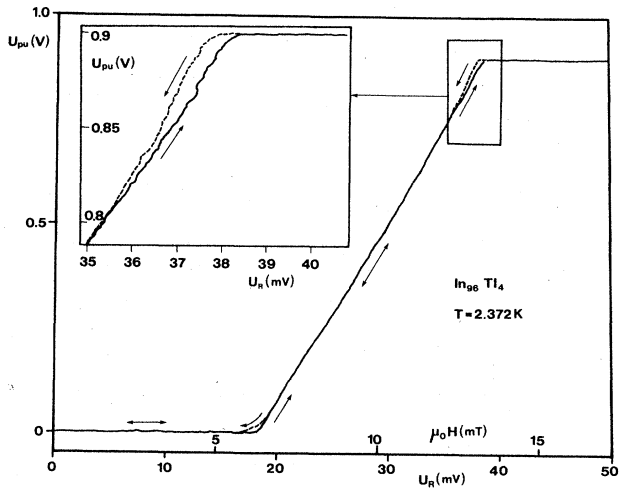

FIG. 1. Recorder tracing of a magnetization cycle in $In_{96}Tl_4$. (U_{pu} represents voltage from the pick-up coil after amplification by an EG&G 128A lock-in amplifier, U_R represents voltage across a precision resistor in the current loop of a superconducting magnet.)

TABLE I. Material parameters.

Sample	Tl concentration (at. %) (±0.1)	T_c (K) (±2 mK)	$\mu_0 H_c(0)$ (mT) (±50 μT)	λ (Ref. 17)
0		3.424	28.08	0.805
1	0.7	3.388	28.12	
2	2.0	3.350	27.92	
3	4.0	3.315	27.75	
4	6.0	3.290	27.68	
5	10.0	3.281	27.80	0.850

large number of experimental runs on the same sample we estimate the accuracy of $H_c(T)$ data to be ± 50 μT. A summary of material parameters is listed in Table I.

III. THEORY

In this section we wish to summarize briefly the equations needed for the present analysis and use the formalism developed in Refs. 9 and 19–23 ($\hbar = k_B = 1$). In order to calculate the thermodynamic properties of a superconductor the full nonlinear Eliashberg equations have to be solved. In the isotropic case they have the following form on the imaginary axis:

$$\tilde{\omega}_n = \omega_n + \pi T \sum_m \lambda(m-n) \frac{\tilde{\omega}_m}{(\tilde{\omega}_m^2 + \tilde{\Delta}_m^2)^{1/2}} + \pi(t_+ + t_-) \frac{\tilde{\omega}_n}{(\tilde{\omega}_n^2 + \tilde{\Delta}_n^2)^{1/2}} , \tag{1}$$

$$\tilde{\Delta}_n = \pi T \sum_m [\lambda(m-n) - \mu^*] \frac{\tilde{\Delta}_m}{(\tilde{\omega}_m^2 + \tilde{\Delta}_m^2)^{1/2}} + \pi(t_+ - t_-) \frac{\tilde{\Delta}_n}{(\tilde{\omega}_n^2 + \tilde{\Delta}_n^2)^{1/2}} , \tag{2}$$

where the ω_n's represent the Matsubara frequencies,

$$\omega_n = \pi T(2n+1) \text{ with } n = 0, \pm 1, \pm 2, \ldots , \tag{3}$$

$$\lambda(m-n) = 2 \int_0^\infty \frac{\omega \alpha^2 F(\omega)}{\omega^2 + (\omega_m - \omega_n)^2} d\omega , \tag{4}$$

μ^* is the Coulomb interaction pseudopotential, and

$$t_+ = \frac{1}{2\pi\tau_n} , \tag{5}$$

$$t_- = \frac{1}{2\pi\tau_p} . \tag{6}$$

τ_n and τ_p are the mean lifetimes of the electronic excited states due to normal and spin-flip scattering, respectively.

The difference in free energy between the superconducting and the normal state is given by[23]

$$\Delta F(T) = \pi T N(0) \sum_n [(\tilde{\omega}_n^2 + \tilde{\Delta}_n^2)^{1/2} - \tilde{\omega}_n^2] \times \left[1 - \frac{\tilde{\omega}_{n0}}{(\tilde{\omega}_n^2 + \tilde{\Delta}_n^2)^{1/2}} \right] , \tag{7}$$

where the

$$\tilde{\omega}_{n0} = \omega_n + \pi T \sum_m \lambda(m-n) \text{sgn}\omega_m + \pi(t_+ + t_-) \text{sgn}\omega_n , \tag{8}$$

are the renormalized normal state frequencies and $N(0)$ is the electronic density of states at the Fermi surface.

From Eqs. (7) and (8) the thermodynamic critical field $H_c(T)$ and the deviation function $D(t)$ are obtained in the following way:

$$H_c(T) = \left[\frac{2}{\mu_0} \right]^{1/2} [\Delta F(T)]^{1/2} \tag{9}$$

and

$$D(T) = \frac{H_c(T)}{H_c(0)} - (1-t^2), \quad t = \frac{T}{T_c} . \tag{10}$$

On the other hand, the critical temperature T_c can be calculated from the linearized Eliashberg equations:

$$\tilde{\omega}_n = \omega_n + \pi T_c \sum_m \lambda(m-n) \text{sgn}\omega_m + \pi(t_+ + t_-) \text{sgn}\omega_n , \tag{11}$$

$$\tilde{\Delta}_n = \pi T_c \sum_m [\lambda(m-n) - \mu^*] \frac{\tilde{\Delta}_m}{|\tilde{\omega}_m|} + \pi(t_+ - t_-) \frac{\tilde{\Delta}_n}{|\tilde{\omega}_n|} . \tag{12}$$

In order to introduce anisotropy effects we use a separable model for the pairing interaction[2]

$$[\alpha^2(\omega) F(\omega)]_{\mathbf{k}\mathbf{k}'} = (1 + a_{\mathbf{k}}) \alpha^2(\omega) F(\omega) (1 + a_{\mathbf{k}'}) \tag{13}$$

and obtain for the critical temperature T_c the anisotropic form of Eqs. (11) and (12) in the following way:[21]

$$\tilde{\omega}_{n,\mathbf{k}} = \omega_n + (1 + a_{\mathbf{k}}) \pi T_c \sum_m \lambda(m-n) \omega_m + \pi(t_+ + t_-) \text{sgn}\omega_n , \tag{14}$$

$$\tilde{\Delta}_{n,\mathbf{k}} = (1 + a_{\mathbf{k}}) \pi T_c \sum_m \lambda(m-n) \left\langle \frac{(1 + a_{\mathbf{k}}) \tilde{\Delta}_{m,\mathbf{k}}}{|\tilde{\omega}_{m,\mathbf{k}}|} \right\rangle - \mu^* \pi T_c \sum_m \left\langle \frac{\tilde{\Delta}_{m,\mathbf{k}}}{|\tilde{\omega}_{m,\mathbf{k}}|} \right\rangle + \pi(t_+ - t_-) \left\langle \frac{\tilde{\Delta}_{n,\mathbf{k}}}{|\tilde{\omega}_{n,\mathbf{k}}|} \right\rangle , \tag{15}$$

where the large angular brackets denote averages over the Fermi surface. Equations (14) and (15) are solved using an iteration procedure and the following simple ansatz for the gap function $\tilde{\Delta}_{n,\mathbf{k}}$:

$$\tilde{\Delta}_{n,\mathbf{k}}=\tilde{\Delta}_{n,0}+a_{\mathbf{k}}\tilde{\Delta}_{n,1}\ , \tag{16}$$

where $\tilde{\Delta}_{n,0}$ and $\tilde{\Delta}_{n,1}$ are assumed to be isotropic. To characterize $a_{\mathbf{k}}$, a simple distribution function $P(a)$ is used,

$$P(a)=\tfrac{1}{2}\delta(-a)+\tfrac{1}{2}\delta(a)\ , \tag{17}$$

where $P(a)da$ denotes the probability for $a_{\mathbf{k}}$ to lie between a and $a+da$. Equation (17) essentially divides the gap function into two parts differing by $\pm a\tilde{\Delta}_{n,1}$.

Concerning the free-energy difference and, hence, $H_c(T)$ the full nonlinear anisotropic Eliashberg equations have to be solved. In order to do that, the formalism of Fermi-surface harmonics (FSH) was introduced into Eqs. (1), (2), (4), and (7). However, because of our simple model for the anisotropy, an equivalent description to Eqs. (16) and (17) is obtained by restriction to zeroth-order FSH in any Fermi-surface subregion. As a final remark we wish to point out that throughout the analysis the parameter t_- characterizing spin-flip scattering events was set equal to zero because of the absence of magnetic impurities.

IV. RESULTS AND ANALYSIS

A. Transition temperature T_c

The experimental results on the change of T_c with Tl concentration show a continuous decrease of T_c (Fig. 2). In order to analyze the data within the theoretical framework outlined in Sec. III, the following problem has to be overcome.[13] Equations (11) and (12) for the transition temperature contain (in addition to λ, which is taken from tunneling results[17]) two unknown quantities, viz., μ^* and t_+ ($t_-=0$). μ^* is obtained in the usual way by fitting the results to the experimental transition temperature in the clean limit ($t_+=0$) and keeping it constant further on. Unfortunately, t_+ which is inversely proportional [Eq. (5)] to the lifetime τ_n of electronic excited states due to momentum scattering at the impurity sites, is inaccessible to experiment. However, based on the reasonable assumption, that τ_n is proportional to the transport scattering time τ_{tr} and, hence, t_+ is proportional to the impurity concentration at low impurity contents, one normalization point of T_c for an impure sample [e.g., In2 in Fig. 2(a)] is sufficient to determine the constant of proportionality. Thus, the entire dependence of T_c on the impurity concentration can be calculated for different values of the anisotropy parameter $\langle a^2\rangle$. Results of this analysis are shown in Fig. 2(a), the best agreement between theory and experiment is obtained for $\langle a^2\rangle=0.04$.

Because the choice of the normalization point is somewhat arbitrary, one has to check how the result is influenced by this choice. There are two possibilities: First, T_c of the sample with the lowest impurity content (In1) is used for the normalization and the best agreement is found for $\langle a^2\rangle=0.035$ rather than for 0.040 [Fig. 2(b)].

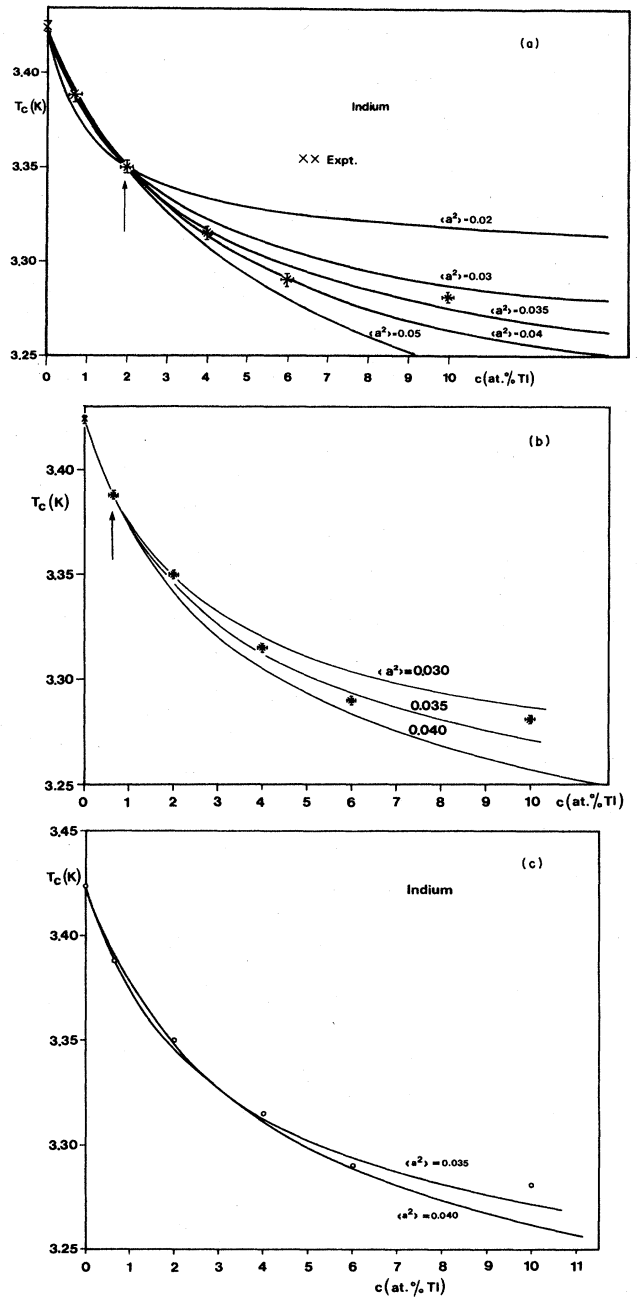

FIG. 2. Change of transition temperature T_c with Tl concentration. The solid lines represent solutions of the linearized anisotropic Eliashberg equations for different values of the anisotropy parameter $\langle a^2\rangle$. (a) Normalization point, In1; (b) In2; (c) average of samples In1, In2, In3, and In4.

Second, constants of proportionality are calculated for four samples (In1, In2, In3, and In4) and their average is used for the analysis [Fig. 2(c)]. In this case the standard deviation of all the experimental data (except for In5) is only 3 mK for $\langle a^2\rangle=0.035$ and 2.8 mK for $\langle a^2\rangle=0.04$. (In5 is not included in this analysis because of the known change of coupling strength and possible nonlinearities of the scattering potentials due to the relatively high-impurity content.)

In summary, the analysis of the T_c depression in indium by the addition of Tl impurities in terms of the linearized anisotropic Eliashberg equations and using the model potential (13) for the electron-phonon coupling anisotropy yields an anisotropy parameter $0.035 \leq \langle a^2 \rangle \leq 0.040$ for pure indium.

B. Thermodynamic critical fields $H_c(T)$ and deviation function $D(t)$

Thus, having established the magnitude of the electron-phonon coupling anisotropy $\langle a^2 \rangle$ in the pure material from the T_c depression, *no* free parameter is involved in the solution of the full anisotropic Eliashberg equations to calculate the temperature dependence of the thermodynamic critical field $\mu_0 H_c(T)$ and the deviation function $D(t)$ for pure indium. The results of these calculations for the deviation function with $\langle a^2 \rangle = 0.035$ and 0.040 as well as for the isotropic case ($\langle a^2 \rangle = 0$) and the weak-coupling BCS limit are shown in Fig. 3(a) together with the experimental data, which were obtained in a temperature range from 30 mK ($t^2 \sim 1 \times 10^{-4}$) to T_c. Clearly, the experiments are incompatible with either the isotropic calculations or the BCS approximation. Unfortunately, the experimental error bars for $D(t)$ are too large to enable a distinction between different values of the anisotropy parameter $\langle a^2 \rangle$ in the range of interest, a problem which seems to be inherent to the evaluation of $D(t)$. For example, for the minimum of $D(t)$ we obtain -0.0253 ± 0.0033, i.e., an error of $\pm 13\%$, in spite of the rather accurate experimental determination of temperatures and fields [$\Delta T = \pm 3$ mK, $\Delta T_c = \pm 2$ mK, $\Delta \mu_0 H_c(T) = \pm 80$ μT, $\Delta \mu_0 H_c(0) = \pm 50$ μT]. Still, the agreement between theory and experiment is very good, if the $\langle a^2 \rangle$ values deduced from the T_c depression are used. This good agreement is further emphasized by considering the results on the 10% Tl alloy presented in Fig. 3(b), which, based on the concept of anisotropy removal, were obtained by solving the *isotropic* Eliashberg equations using the appropriate $\alpha^2 F(\omega)$ spectrum (see Table 1 and Fig. 6) for $In_{90}Tl_{10}$.

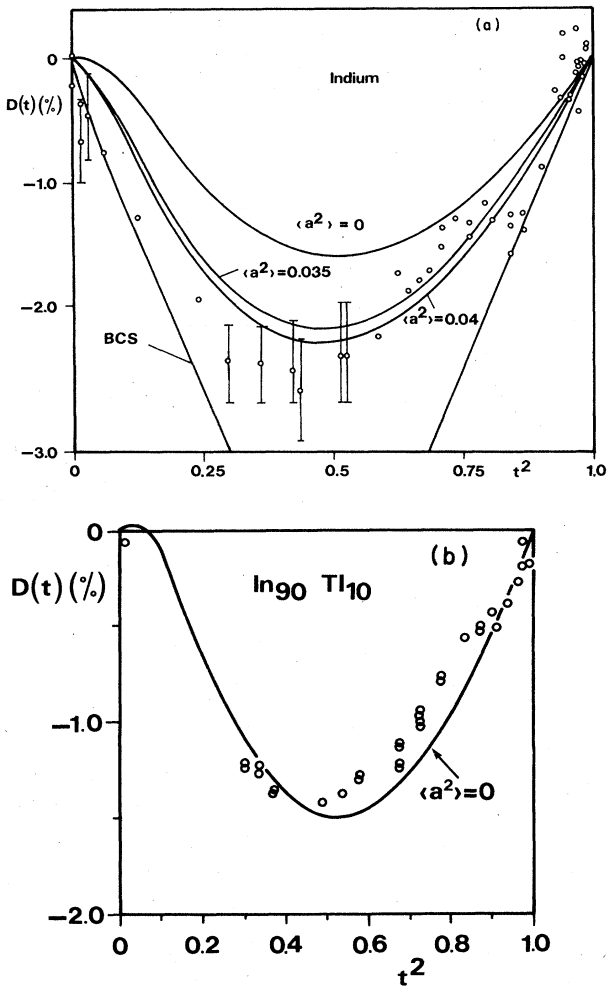

FIG. 3. Deviation function of (a) pure In and (b) $In_{90}Tl_{10}$.

As a final consistency check the absolute value of $\mu_0 H_c(0)$ for pure In, which was measured directly and found to be (28.08 ± 0.05) mT, can be compared with theory for different values of $\langle a^2 \rangle$. The corresponding results for $\langle a^2 \rangle = 0$, 0.035, and 0.040 are 28.75, 28.21, and 28.13 mT, respectively, which show again best agreement for $\langle a^2 \rangle = 0.04$. We wish to point out, however, that the absolute values of $\mu_0 H_c(T)$ according to Eqs. (7) and (9) depend directly on the density of states at the Fermi level, which has to be calculated from the Sommerfeld constant γ of the electronic specific heat. The values $\mu_0 H_c(0)$ quoted above were obtained with $\gamma = 1.69$ ($\pm 0.5\%$) mJ mole^{-1} K^{-2},[16] which is, according to our knowledge, the most accurate γ value for pure indium obtained calorimetrically. Nevertheless, the small experimental error of $\pm 0.5\%$ in γ produces an uncertainty of ± 70 μT in $\mu_0 H_c(0)$.

In summary, both the analysis of the deviation function and of the thermodynamic critical field at $T = 0$ for pure indium support the conclusion of Sec. IV A, viz., that the anisotropy parameter $\langle a^2 \rangle$ in pure indium lies between 0.035 and 0.040.

Starting from this value the smearing out of anisotropy in the other samples can be represented in the following way. From the solution of the anisotropic Eliashberg equations for the gap parameter the rms value of the gap anisotropy $\langle R^2 \rangle^{1/2}$ is obtained,

$$\langle R^2 \rangle^{1/2} = \left[\frac{\sum_n (\langle \bar{\Delta}_{n,k}^2 \rangle - \langle \bar{\Delta}_{n,k} \rangle^2)}{\sum_n \langle \bar{\Delta}_{n,k}^2 \rangle} \right]^{1/2}, \quad \bar{\Delta}_{n,k} = \frac{\tilde{\Delta}_{n,k}}{|\tilde{\omega}_n|}, \tag{18}$$

which is related to the parameter $\langle a^2 \rangle$ of the coupling anisotropy according to our calculations for *pure* In by

$$\frac{\langle R^2 \rangle^{1/2}}{\langle a^2 \rangle^{1/2}} = 0.77 . \tag{19}$$

Assuming that this ratio remains constant, the results for $\langle a^2 \rangle$ are shown in Fig. 4, which demonstrates that anisotropy effects become negligibly small for Tl concentrations exceeding about 6 at. % in this system.

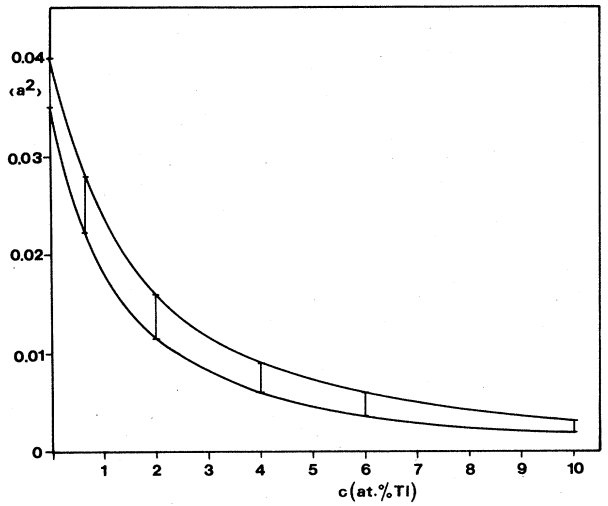

FIG. 4. Assignment of $\langle a^2 \rangle$ values to each sample via the anisotropic gap function starting from the $\langle a^2 \rangle$ range 0.035—0.040 for pure indium.

C. Influence of experimental uncertainties in T_{c0} and c_{Tl}

From the analysis presented in the preceding sections we note that some experimental quantities are needed as input parameters for the theory, in particular, the transition temperature of pure indium T_{c0} to determine μ^*, and the impurity concentration c_{Tl} (and the corresponding T_c) to determine the proportionality constant between τ_n and τ_{tr}. In order to check the influence of experimental uncertainties in T_{c0}, T_{ci}, and c_{Tl} on our conclusions concerning the anisotropy parameter $\langle a^2 \rangle$, several theoretical runs were made using extreme values of our error limits for one input parameter and keeping the others constant. For instance, if we reduce T_{c0} by 3 mK, the maximum increase of the calculated transition temperatures occurs at high Tl concentrations and amounts to 2.5 and 3 mK for In4 and In5, respectively. The effect of Δc_{Tl}, which is shown in Fig. 5, has the same order of magnitude. In summary, we find that changes of these input parameters within the experimental error limits do not affect our conclusions on $\langle a^2 \rangle$.

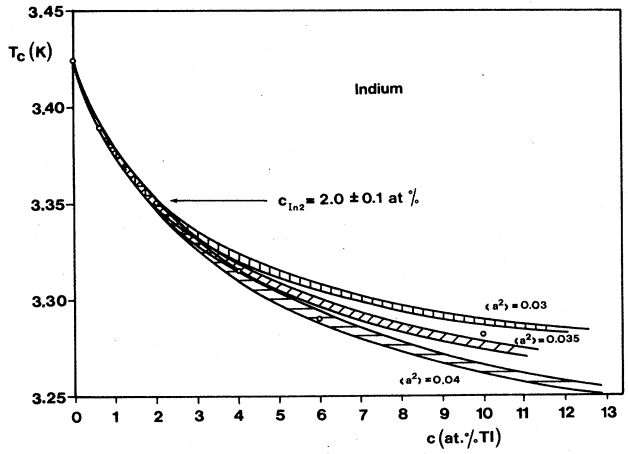

FIG. 5. Influence of experimental uncertainties in the Tl concentration c_{Tl} on the theoretical analysis for various values of $\langle a^2 \rangle$.

D. Functional derivatives

In order to further analyze the influence of input parameters on our results, the basic input parameter of the Eliashberg equations, viz., the spectral function $\alpha^2 F(\omega)$, is discussed in terms of functional derivatives.[20] The spectral functions for pure indium and $In_{90}Tl_{10}$, which were taken from Ref. 17 and were available in the form of 80 (82) data pairs in the energy range $0 \leq \hbar\omega \leq 15.8$ (16.2) meV are shown in Fig. 6. It will be noted, that no dramatic shifts of the functions with impurity concentration occur, which again demonstrates that the system InTl is very favorable for the present analysis.

The functional derivative of the transition temperature for pure In is similar to results obtained on other superconductors and has been calculated previously by Daams and Carbotte.[9] It shows a peak at about 2.5 meV and decreases slowly towards higher energies. In order to deduce specific results on the change of transition temperature with impurity concentration (as shown in Fig. 2) including variations of the spectral function, three cases were considered. First, we assume that one data point at the first peak (6.6 meV) of the spectral function is too low by 1%. Using this "new" spectrum the whole procedure described in Sec. IV A was repeated. The data show, that the changes of T_c in the whole concentration range are always smaller than 0.1 mK. In the second and third case, we assume that the entire spectrum is wrong by 1% and 5%, respectively. The corresponding changes of T_c are ≤ 0.7 and ≤ 3.0 mK, respectively, which is in both cases smaller than the experimental uncertainties and, hence, does not affect our analysis.

Another point of interest is the choice of the cutoff fre-

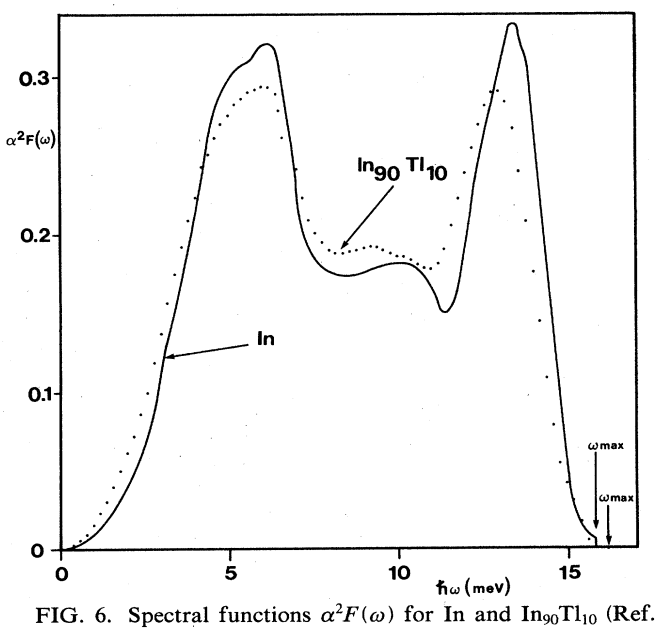

FIG. 6. Spectral functions $\alpha^2 F(\omega)$ for In and $In_{90}Tl_{10}$ (Ref. 17).

quency ω_c used in the T_c calculation from the Eliashberg equations. An increase of ω_c from the usual value of $3\omega_{max}$ reduces the rms difference between theory and experiment [Fig. 2(c)] from 2.8 to 2.4 mK ($\langle a^2\rangle=0.04$), which is considered to be insignificant and not worth the considerably increasing computing times.

Similar calculations of functional derivatives were made for the deviation function $D(t)$.[24] The results are shown in Fig. 7 as a function of t^2 with the energy of the spectral function, where the change in $\alpha^2F(\omega)$ occurs, as a parameter. It will be noted, that pronounced minima of the derivatives occur at very low energies only in almost the entire temperature range. However, because $\alpha^2F(\omega)$ itself is extremely small at these low energies we immediately expect that the influences of changes in $\alpha^2F(\omega)$ on $D(t)$ will be negligibly small. In order to prove this conclusion, the same assumptions were made as above and the changes of $D(t)$ evaluated at $t=0.7$, i.e., near the minimum of $D(t)$. Changing $\alpha^2F(\omega)$ by 1% and 5%, respectively, and repeating the entire calculation (including the readjustment of μ^* to the new spectra) results in variations of the minimum of $D(t)$ by less than 2×10^{-4} and 7×10^{-4}, respectively. Similarly, functional derivatives were calculated for the thermodynamic critical field at zero temperature, the corresponding results affect $\mu_0H_c(0)$ by less than 10 and 30 μT, respectively. Clearly, all these changes are much smaller than the experimental error bars and can, therefore, be neglected.

Finally, the influence of the cutoff frequency ω_c on the theoretical result for $\mu_0H_c(0)$ was investigated in one case. An increase of ω_c from $3\omega_{max}$ to $6\omega_{max}$ increases $\mu_0H_c(0)$ by 0.1 mT, which is comparable to the experimental error bar. However, because of the prohibitively long computing times all of the calculations had to be made with $\omega_c=3\omega_{max}$.

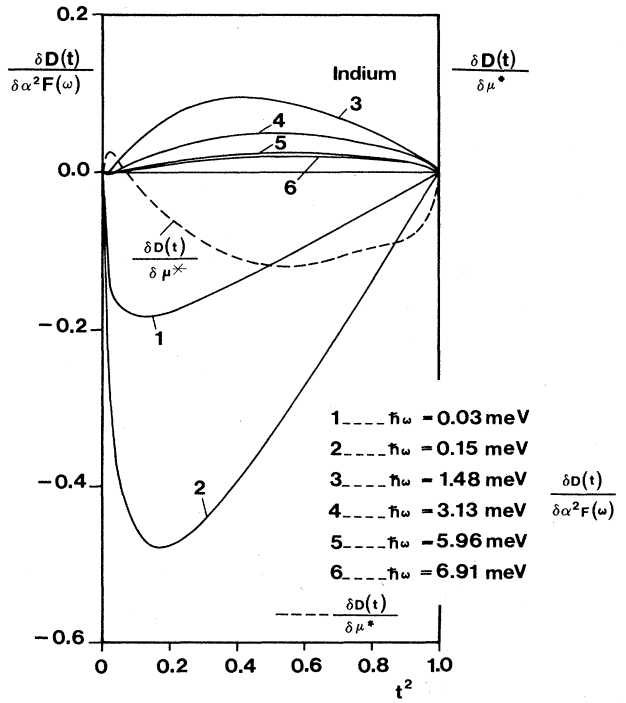

FIG. 7. Functional derivatives of the deviation function in pure indium.

E. The function μ^*

All of the results presented as yet confirm the existence of a rather large electron-phonon coupling anisotropy in pure indium and the concept of anisotropy removal due to impurity scattering in a very clear and consistent way. In order to emphasize this conclusion even further we wish to discuss in this section alternative mechanisms, which could lead to changes of T_c and $\mu_0H_c(0)$ in our samples, in particular, variations of the Coulomb interaction pseudopotential μ^* and the electron-phonon coupling strength λ. Experimentally, $\alpha^2F(\omega)$ spectra are available for pure indium and the alloy $In_{90}Tl_{10}$ (cf. Fig. 6), the coupling constant λ changes in these two materials from 0.805 to 0.850.[17]

In order to analyze the experimental T_c variation, several possibilities for the change of the coupling strength were tested and used to calculate μ^* values, which reproduce the experimental T_c curve (Fig. 2). The results of these calculations are shown in Fig. 8 and may be summarized as follows.

(1) We assume that there is no coupling anisotropy ($\langle a^2\rangle=0$) and no change in λ. In this case μ^* increases by 7.3% for $In_{90}Tl_{10}$ and, of course, yields a wrong result for the 10% alloy.

(2) Assuming again $\langle a^2\rangle=0$ we calculate μ^* for a linear variation of λ between 0.805 and 0.850 according to the impurity concentration (i.e., by multiplying each data point of the α^2F spectrum of pure indium by the appropriate factor). In this case, μ^* increases by 29.2%; the

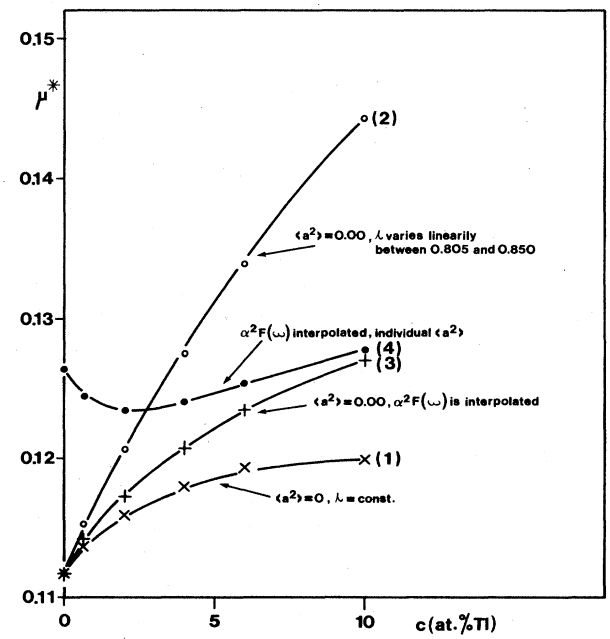

FIG. 8. Variation of μ^* ($\omega_c=3\omega_{max}$) obtained under various assumptions to describe the experimental T_c variation.

result for the 10% alloy is erroneous, because the spectrum is not reproduced correctly by this procedure.

(3) Using again $\langle a^2 \rangle = 0$, each data point of the $\alpha^2F(\omega)$ spectra was interpolated linearly according to the impurity concentration and the calculation repeated with these individual spectra. In this case, μ^* increases by 13.8%.

(4) Using these interpolated $\alpha^2F(\omega)$ spectra and the anisotropy parameters $\langle a^2 \rangle$ assigned to each sample according to the discussion presented in Sec. IV B [Eqs. (18) and (19), and Fig. 4], μ^* varies within $\pm 1.8\%$ only. The corresponding μ^* values for the pure sample and the 10% alloy, respectively, which are not affected by interpolation errors, but contain our results on $\langle a^2 \rangle$, viz. $\langle a^2 \rangle = 0.040$ and 0.003, are 0.1263 and 0.1278, respectively.

In view of the physical meaning of μ^*, which describes the long-ranging part in the Coulomb repulsion, and considering the small changes in the $\alpha^2F(\omega)$ spectra (Fig. 6), a variation of μ^* by as much as 10% is extremely unlikely. On the contrary, the almost constant μ^* values obtained from the anisotropic calculations comply very well with the physical meaning of μ^*. We believe, that the initial slight drop of μ^* in the anisotropic calculations is artificial and caused by our linear interpolation scheme for $\alpha^2F(\omega)$, because changes of the spectral functions at low impurity concentrations are very unlikely also. An additional uncertainty comes from the error bars related to the $\langle a^2 \rangle$ assignments (cf. Fig. 4).

As a final consistency check the thermodynamic critical fields at zero temperature $\mu_0 H_c(0)$ were calculated for the following cases. (i) The anisotropic Eliashberg equations were solved for all the samples using the interpolated spectral functions, an $\langle a^2 \rangle$ value of 0.04 for pure indium, and the assigned $\langle a^2 \rangle$ values for the other samples according to Eqs. (18), (19), and Fig. 4. (ii) Because of the uncertainties associated with the interpolation of the spectral functions and with the assignment of $\langle a^2 \rangle$ values to the impure samples the anisotropic Eliashberg equations were solved for an anisotropy parameter of 0.040 and 0.035 for pure indium, respectively, and with the original spectral function for pure indium, but using the appropriate lifetimes of the electronic excited states according to the impurity concentration. (iii) The isotropic Eliashberg equations were solved using again the interpolated spectral functions and the μ^* values shown in Fig. 8 [assumption (3)]. In all the calculations the Sommerfeld constant γ of the electronic specific heat was kept constant [which could lead to small errors in the absolute values of $H_c(0)$ as a function of impurity concentration, but cannot be avoided because of the lack of experimental data]; furthermore, a constant correction term of 0.1 mT was included to account for the influence of the cutoff frequency ω_c (cf. Sec. IV D). A summary of these results is shown in Fig. 9, the relatively large uncertainties in the calculations are introduced by the experimental error bar for the Sommerfeld constant ($\pm 0.5\%$, Ref. 16). Again, the general agreement between the anisotropic calculations and experiment is very satisfactory, especially at low-impurity concentrations where the differences between isotropic and anisotropic calculations are largest. Concerning the anisotropic calculations we find the best agreement for the cases (i) and (ii) (with $\langle a^2 \rangle = 0.035$), where the standard deviation of all the data up to an impurity concentration of 6 at. % amounts only to 0.11 and 0.13 mT, respectively. Furthermore, the close agreement between the theoretical results based on calculations for "clean" superconductors with varying anisotropy parameter [case (ii)] and for an anisotropic starting material with increasing impurity concentration [case (iii)] is considered again as evidence for the consistency of the anisotropy removal concept.

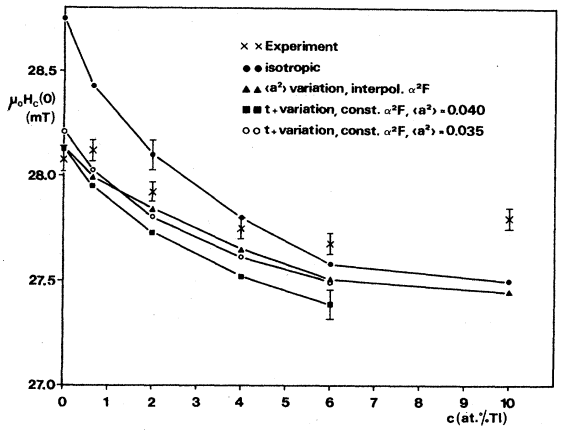

FIG. 9. Thermodynamic critical field $\mu_0 H_c(0)$ as a function of Tl concentration. γ is kept constant throughout the calculations, a correction for $\omega_c = 6\omega_{\max}$ is included.

V. CONCLUSIONS

From the experimental results on the thermodynamics of the type-I superconductor indium and several InTl alloys, which were obtained in the temperature range from 30 mK to T_c, combined with an extensive analysis in terms of Eliashberg theory, we were able to show, that a consistent description of results is achieved only, if anisotropy effects of the electron-phonon coupling are included. Using a separable model potential and a simple distribution function for the coupling anisotropy, an anisotropy parameter $0.035 \leq \langle a^2 \rangle \leq 0.040$ has to be invoked for pure indium. The analysis shows that the T_c depression with increasing impurity concentration is the most sensitive tool for the determination of $\langle a^2 \rangle$, together with a direct comparison of the thermodynamic critical field at zero temperature. The analysis in terms of the deviation function suffers from the comparatively large experimental error bars and is not too sensitive to small changes of the anisotropy parameter $\langle a^2 \rangle$.

A thorough discussion of the effect of input parameters on our theoretical analysis as well as attempts to ascribe the experimental data to alternative physical mechanisms, e.g., variations of the coupling strength and the Coulomb repulsion, show consistently that the concept of coupling anisotropy removal due to impurity scattering is valid in the present system.

ACKNOWLEDGMENTS

We wish to thank H. Niedermaier for his expert technical help, J. Schmiedmayer and H. Wiesinger for their par-

ticipation in some experiments, and P. Wobrauschek for taking the x-ray fluorescence data. We are grateful to J. M. Daams and J. P. Carbotte for providing us with their Eliashberg-theory programs in FSH notation. The calculations were performed on the UNIVAC 1100/81 computer of the Elektronische Datenverarbeitungszentrum, Technische Universität Graz. This work was supported in part by Fonds zur Förderung der wissenschaftlichen Forschung, Wien, under Contract No. 3973.

[1]P. W. Anderson, J. Phys. Chem. Solids **11**, 26 (1959).
[2]D. Markowitz and L. P. Kadanoff, Phys. Rev. **131**, 563 (1963).
[3]J. R. Clem, Ann. Phys. **40**, 268 (1966).
[4]D. K. Finnemore and D. E. Mapother, Phys. Rev. **140**, A507 (1965).
[5]D. U. Gubser, Phys. Rev. B **6**, 827 (1972).
[6]A. J. Bennet, Phys. Rev. **140**, A1902 (1965).
[7]C. R. Leavens and J. P. Carbotte, Ann. Phys. **70**, 338 (1972).
[8]J. P. Carbotte, in *Anisotropy Effects in Superconductors,* edited by H. W. Weber (Plenum, New York, 1977), p. 183.
[9]J. M. Daams and J. P. Carbotte, J. Low Temp. Phys. **43**, 263 (1981).
[10]W. H. Butler and P. B. Allen, in *Superconductivity in d- and f-Band Metals,* edited by D. H. Douglas (Plenum, New York, 1976), p. 73.
[11]J. L. Bostock and M. L. A. Mac Vicar, in *Anisotropy Effects in Superconductors,* edited by H. W. Weber (Plenum, New York, 1977), p. 213.
[12]E. Moser, E. Seidl, and H. W. Weber, J. Low Temp. Phys. **49**, 585 (1982).
[13]E. Moser, P. Hahn, E. Seidl, H. W. Weber, and E. Schachinger, in *Superconductivity in d- and f-Band Metals,* edited by W. Buckel and W. Weber (Kernforschungszentrum, Karlsruhe, 1982), p. 519.
[14]M. F. Merriam, J. Hagen, and H. L. Luo, Phys. Rev. **154**, 424 (1967).
[15]D. U. Gubser, D. E. Mapother, and D. L. Connelly, Phys. Rev. B **2**, 2547 (1970).
[16]H. R. O'Neal and N. E. Phillips, Phys. Rev. **137**, A748 (1965).
[17]R. C. Dynes and J. M. Rowell, Tabulation of the Electron-Phonon Interaction, Part I, Bell Laboratories, Murray Hill (unpublished).
[18]V. Gutmann and E. Hengge, *Allgemeine und Anorganische Chemie* (Verlag Chemie, Weinheim, 1982), p. 83.
[19]G. Bergmann and D. Rainer, Z. Phys. **236**, 59 (1973).
[20]D. Rainer and G. Bergmann, J. Low Temp. Phys. **14**, 501 (1974).
[21]J. M. Daams, E. Schachinger, and J. P. Carbotte, J. Low Temp. Phys. **42**, 69 (1981).
[22]P. B. Allen, Phys. Rev. B **13**, 1416 (1976).
[23]J. Bardeen and M. J. Stephen, Phys. Rev. **136**, A1485 (1964).
[24]J. M. Daams and J. P. Carbotte, Can. J. Phys. **56**, 1248 (1978).